LBNL-42956

ERNEST ORLANDO LAWRENCE
BERKELEY NATIONAL LABORATORY

6540

Initial Experimental Verification of the Neutron Beam Modeling for the LBNL BNCT Facility

D.L. Bleuel, W.T. Chu, R.J. Donahue, B.A. Ludewigt,
R.J. McDonald, A.R. Smith, N.A. Stone, and J. Vujic

Environment, Health and Safety Division

January 1999

Presented at the
15th International Conference on the Application of Accelerators in Research and Industry, CAARI '98
Denton, TX,
November 4–7, 1998,
and to be published in
the Proceedings

LBNL-42956

Initial Experimental Verification of the Neutron Beam Modeling for the LBNL BNCT Facility

D.L. Bleuel,[a,b] W.T. Chu,[b] R.J. Donahue,[b] B.A. Ludewigt,[b]
R.J. McDonald,[b] A.R. Smith,[b] N.A. Stone,[a,b] and J. Vujic[a]

[a]Department of Nuclear Engineering
University of California, Berkeley

and

[b]Ernest Orlando Lawrence Berkeley National Laboratory
University of California
Berkeley, California 94720

January 1999

This work was supported by the U.S. Department of Energy under Contract No. DE-AC03-76SF00098.

Initial Experimental Verification of the Neutron Beam Modeling for the LBNL BNCT Facility*

D. L. Bleuel,[a,b] W. T. Chu,[a] R. J. Donahue,[a]
B. A. Ludewigt[a] R. J. McDonald,[a] A. R. Smith,[a] N. A. Stone,[a,b] J. Vujic,[b]
[a]Ernest Orlando Lawrence Berkeley National Laboratory
[b]Department of Nuclear Engineering, University of California
Berkeley, CA 94720

Abstract

In preparation for future clinical BNCT trials, neutron production via the ^{7}Li(p,n) reaction as well as subsequent moderation to produce epithermal neutrons have been studied. Proper design of a moderator and filter assembly is crucial in producing an optimal epithermal neutron spectrum for brain tumor treatments. Based on in-phantom figures-of-merit, desirable assemblies have been identified. Experiments were performed at the Lawrence Berkeley National Laboratory's 88-inch cyclotron to characterize epithermal neutron beams created using several microamperes of 2.5 MeV protons on a lithium target. The neutron moderating assembly consisted of Al/AlF_3 and Teflon, with a lead reflector to produce an epithermal spectrum strongly peaked at 10-20 keV. The thermal neutron fluence was measured as a function of depth in a cubic lucite head phantom by neutron activation in gold foils. Portions of the neutron spectrum were measured by in-air activation of six cadmium-covered materials (Au, Mn, In, Cu, Co, W) with high epithermal neutron absorbtion resonances. The results are reasonably reproduced in Monte Carlo computational models, confirming their validity.

*Supported by the U.S. Department of Energy under Contract No. DE-AC03-76SF00098.

1 Introduction

Boron Neutron Capture Therapy (BNCT) is a binary cancer treatment modality in which a drug containing ^{10}B is administered to a cancer patient, who is subsequently irradiated with an epithermal neutron beam. The primary cancers being studied for BNCT are glioblastoma multiforme, as well as other head and neck cancers and certain melanomas. The drug is preferentially absorbed into cancer cells, leading to a higher concentration of boron in cancer cells than in normal healthy tissue cells. The patient is irradiated by an epithermal neutron beam which produces a thermal neutron distribution in the patient's head. These thermal neutrons are captured by the ^{10}B, which has a high thermal capture cross section, producing two highly energetic particles, a ^{7}Li nucleus and an alpha particle. These particles have a range on order of the dimension of a single cell and, therefore, deliver nearly all their kinetic energy to the cell in which the boron resides.

An accelerator-based BNCT facility is under development at the Lawrence Berkeley National Laboratory (LBNL).[1] The $^{7}Li(p,n)^{7}Be$ reaction at proton energies of about 2.5 MeV will be utilized since it offers a high neutron yield in combination with a low maximum neutron energy. The d.c. accelerator design features an electrostatic quadrupole (ESQ) column which is ideally suited for high beam current and high reliability operation.[2] The accelerator will be able to produce 50 mA of 2.5 MeV protons. A metallic lithium target has been designed which can handle the associated heat load.

Improving BNCT treatments relies on advances in two areas–increasing the boron localization in tumor cells with new boronated drugs, and better tailoring of the epithermal neutron spectrum to more effectively distribute a thermal neutron fluence at pertinent depths in the brain. A great deal of computational modeling at LBNL has yielded improved neutron beam designs with neutrons produced by the $^{7}Li(p,n)$ reaction and various moderator assemblies.[3] To confirm the characteristics of these designs, as well as the accuracy of the Monte Carlo modeling, low intensity experiments were performed at LBNL's 88-inch Cyclotron Center.

2 Accelerator/Moderator Setup

The 88-inch cyclotron was tuned to deliver a beam of ~ 5 μA of H_2^+ ions at 5 MeV onto a natural lithium metal target. Therefore, approximately $6x10^{13}$ protons/sec at 2.5 MeV were delivered to the target. The 7.62 cm diameter circular target was composed of 100 μm of natural lithium vacuum deposited onto a 0.635 cm (1/4") thick copper backing, which in

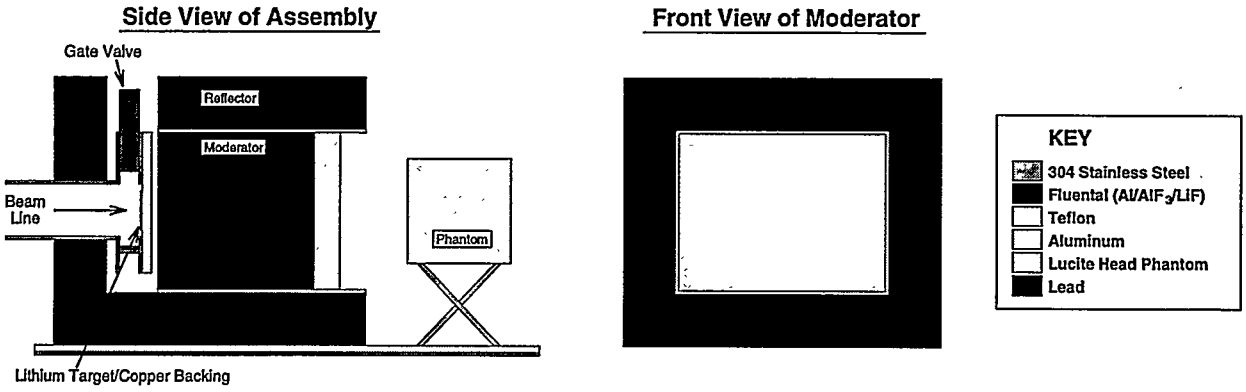

Figure 1: Moderator/Reflector Assembly Setup.

turn was mounted onto the inside back plate of a stainless steel gate valve. For transport, the valve was closed in an argon atmosphere to prevent oxidation of the lithium target and opened again in vacuum. The entire gate valve was electrically isolated from the beam pipe so that the accumulated charge from the proton beam could be measured.

The moderator and reflector were assembled around the target as shown in Fig. 1. The reflector was built around the valve and an aluminum box, with lead bricks giving a thickness of 10 cm thick on all sides. This thickness was chosen as a compromise between optimal neutron reflectivity and the weight load of the table upon which the assembly was built. No lead was added directly above the valve. The aluminum box was included to facilitate easy access to the moderator materials without the need to disassemble the reflector. Two materials were used in the moderator: Fluental and Teflon. Fluental is a mixture of 69% AlF_3, 30% metallic aluminum, and 1% LiF and was developed by the Technical Research Centre of Finland.[4] The Fluental formed a block 30 cm thick, with a height of 30 cm and a width of 40 cm. This block was supplemented by 5 cm of Teflon (CF_2), placed immediately after the 30 cm of Fluental, of the same height and width.

This configuration was shown by Monte Carlo neutronics calculations using MCNP[5] to produce a narrow neutron spectrum centered around $\sim$ 10 keV, as shown in Fig. 2. A beam with such a spectrum is much more penetrating than beams from currently operating reactors.[3]

Such a narrow spectrum, with nearly all neutrons possessing energies between 1 keV and 40 keV, has been shown to be nearly optimal for delivering high tumor doses to the deepest portions of the brain.[6] As can be seen, there has been a significant improvement in this characteristic over previous designs.[3]

Whereas ealier designs included an Al_2O_3 reflector, a lead reflector allows additional tai-

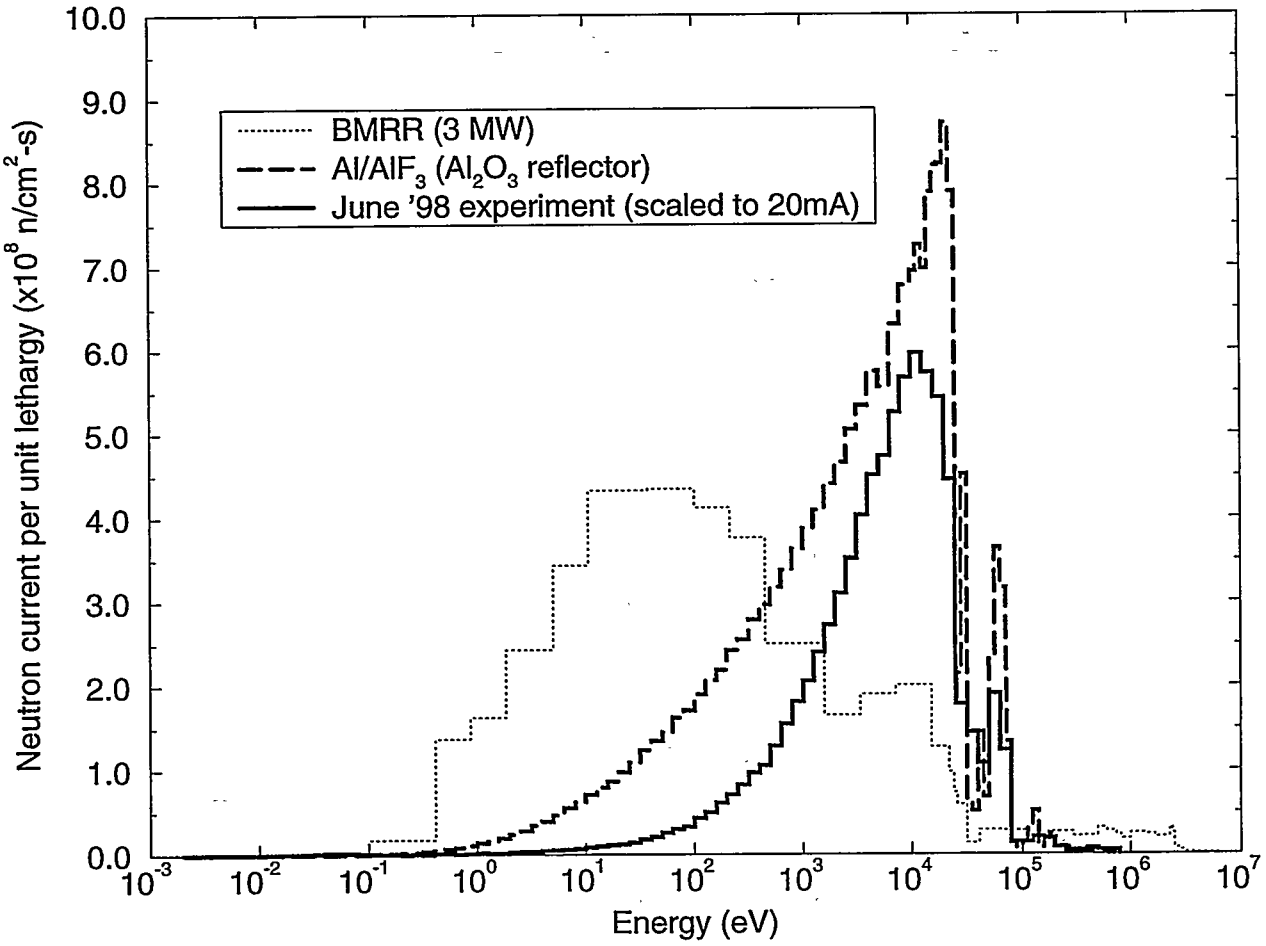

Figure 2: Neutron Current Spectrum of three different beams.

loring of the neutron spectrum to the desired energy range to produce the highest tumor doses at the center of the brain, which is the hardest point to treat. While lead was determined to be a poorer reflector in terms of providing the highest total flux, its high Z allows neutrons to be reflected with almost no loss in energy. This is an important characteristic when designing narrower neutron spectra. Reflected neutrons require less moderation since they travel through more moderator than neutrons closer to the assembly's centerline. Therefore, energy loss in the reflector is less desirable. Al_2O_3 acts similarly to Fluental in its moderating capabilities, whereas lead reflects neutrons with virtually no change in energy. The lower energy tail from previous designs is greatly reduced, producing a narrower spectrum, albeit at a somewhat lower flux. Preliminary studies have shown that an improved spectrum such as this can provide increases in the tumor dose of $\sim$ 10% over the Al_2O_3 reflector design, or $\sim$ 60% better than that produced by the BMRR beam.

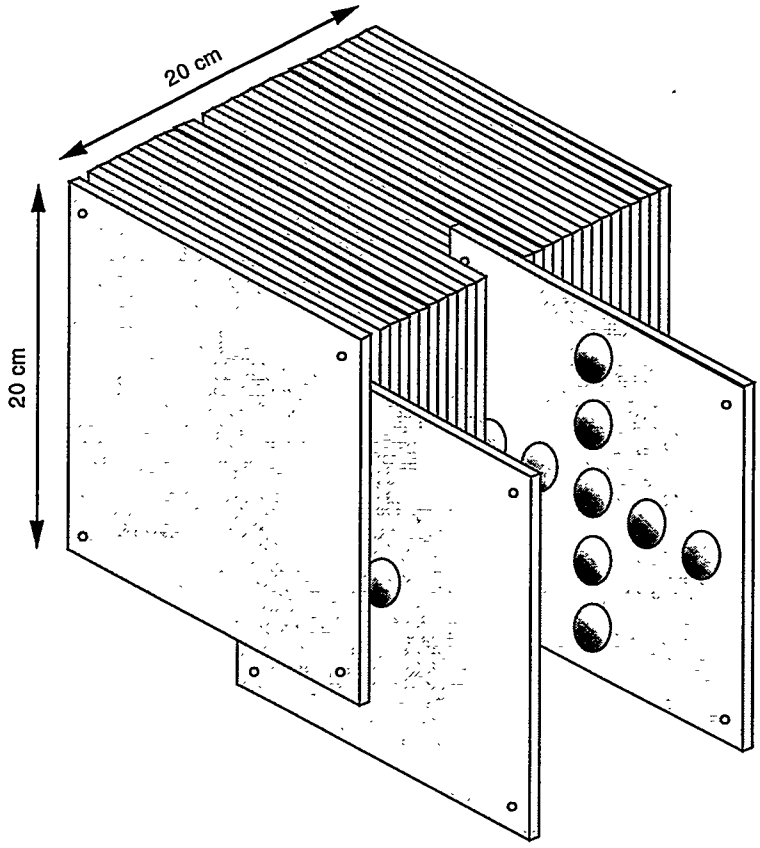

Figure 3: Lucite head phantom with 2.54 cm diameter gold foils. Lucite density = 1.17 g/cm^3. All slabs beyond first have one centered gold foil except for cross patterns at depths of 3.17 cm, 5.08 cm, and 8.26 cm, and four slabs at the back, which contain no foils.

3 In-Phantom Measurements

3.1 Setup

In the first experiment performed, the thermal neutron flux in a head phantom was characterized. This was performed by placing thin gold foils ($\sim$ 500 mg each) in a cubic lucite head phantom, which was positioned 13 cm away from the edge of the moderator, as shown also in Fig. 1. The gold foils were mounted at 0.635 cm (1/4") intervals along the centerline of the phantom. At three positions in the phantom (3.17 cm, 5.08 cm, and 8.26 cm), eight additional foils were mounted in a cross-like pattern to measure the radial thermal neutron distribution. The positions of these foils is shown in Fig 3.

3.2 Measurements

Since neutrons were produced via the ^{7}Li(p,n)^{7}Be reaction, the activity of the ^{7}Be in the target gives a direct and absolute measurement of the number of neutrons produced. Following each exposure, an absolutely calibrated (±5%) germanium gamma-ray spectrometer was brought into the experimental cave and used to measure the ^{7}Be activity using the 478 keV line. The moderator was removed and the activity was measured through the target backing. At a detector distance of about 2 meters, the count-rate was adequate to obtain data in about 10 minutes. Thus, using the observed rate of emitted gamma rays, the absolutely calibrated detector, the absorption correction, and the known branching ratio for 478 keV gamma rays (10.4%), the number of neutrons produced in each run could be determined. The attenuation of 478 keV gamma rays through the target backing was obtained after the experiment by measuring the counting rate from the front of the ^{7}Be target and comparing it to the counting rate measured through the backing.

The gold foils in the phantom were activated via the neutron capture of ^{197}Au producing the 2.7 day ^{198}Au activity. This decay is characterized by a 411 keV gamma ray observed in 95.5% of the decays. The counting was done with a low-background Pb-shielded 20 cm diameter by 10 cm thick NaI detector in the Low-Background Facility at the Berkeley Laboratory. The observed counting rate, corrected for decay time and detector efficiency, was compared with Monte Carlo calculations.

3.3 Results

The total yield thus measured was calculated to be 1.87x10^{13} neutrons over an irradiation time of a little over an hour. MCNP was used to model the full assembly in Fig. 1, with the exception of the aluminum/stainless steel table and the full phantom support stand, although 2 mm of stainless steel was included directly under the phantom. The gold foils were included in the MCNP calculation in order to properly account for thermal depletion in the gold. Activation was determined by multiplying the energy-dependent absorption cross section pointwise by the volume-averaged flux in each gold foil to determine the number of reactions.

Some disagreement was observed between the Monte Carlo model and the experimental measurements in the slopes of the gold foil activation. It was then determined that significant room scatter was occuring and needed to be accounted for in MCNP. Properly accounting for room scatter was difficult. The assembly was rather near ($\sim$ 1 meter) one of the concrete walls on one side, and a little more than a meter from the floor and ceiling. The other walls in

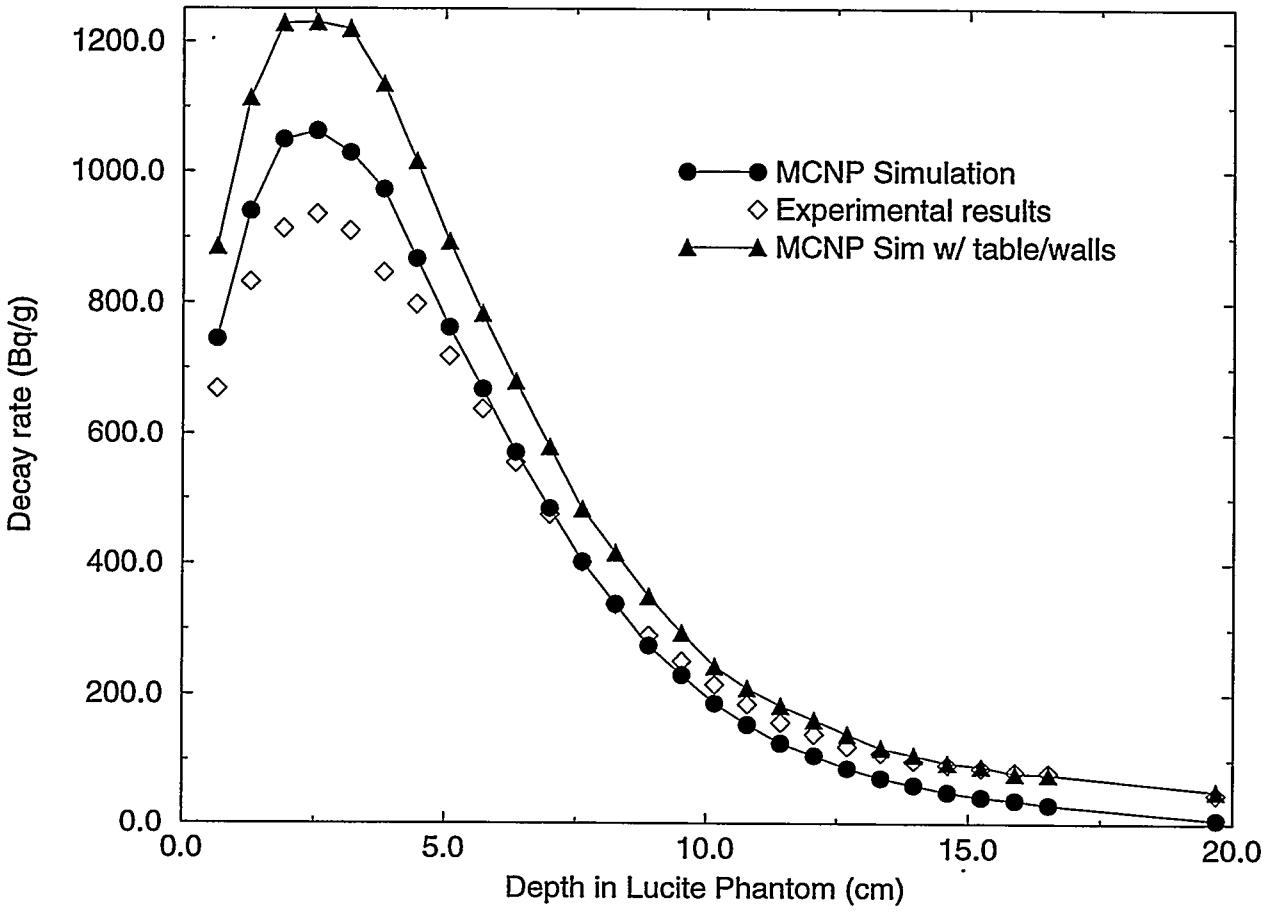

Figure 4: Gold foil activation comparison between MCNP simulation, with and without concrete walls included, and the experimental data. All error bars are on order of or smaller than the size of the data points.

the room were significantly further away. However, many other experiments and supporting equipment occupy the same room, all of which could have contributed to scatter. For the comparison, the floor, ceiling, and walls of the room were added to the MCNP model, as well as the stainless steel and aluminum table. The results, as well as a comparison with the case in which the walls and table are not modeled, are shown in Fig. 4.

The activation in the MCNP calculations were higher than those observed in the experiment by as much as 30% at the peak. This indicated an unaccounted for overestimation of the number of neutrons reaching the phantom. More important than comparing the absolute activation curves is confirming that the slope of each curve is similar. This confirms that the incident neutron spectral shape is as expected, though the total fluence may be different. The curves were thus normalized to each other by multiplying the MCNP results by the ratio of the peaks to set the maximum activation equal to that of the experiment. Fig. 5

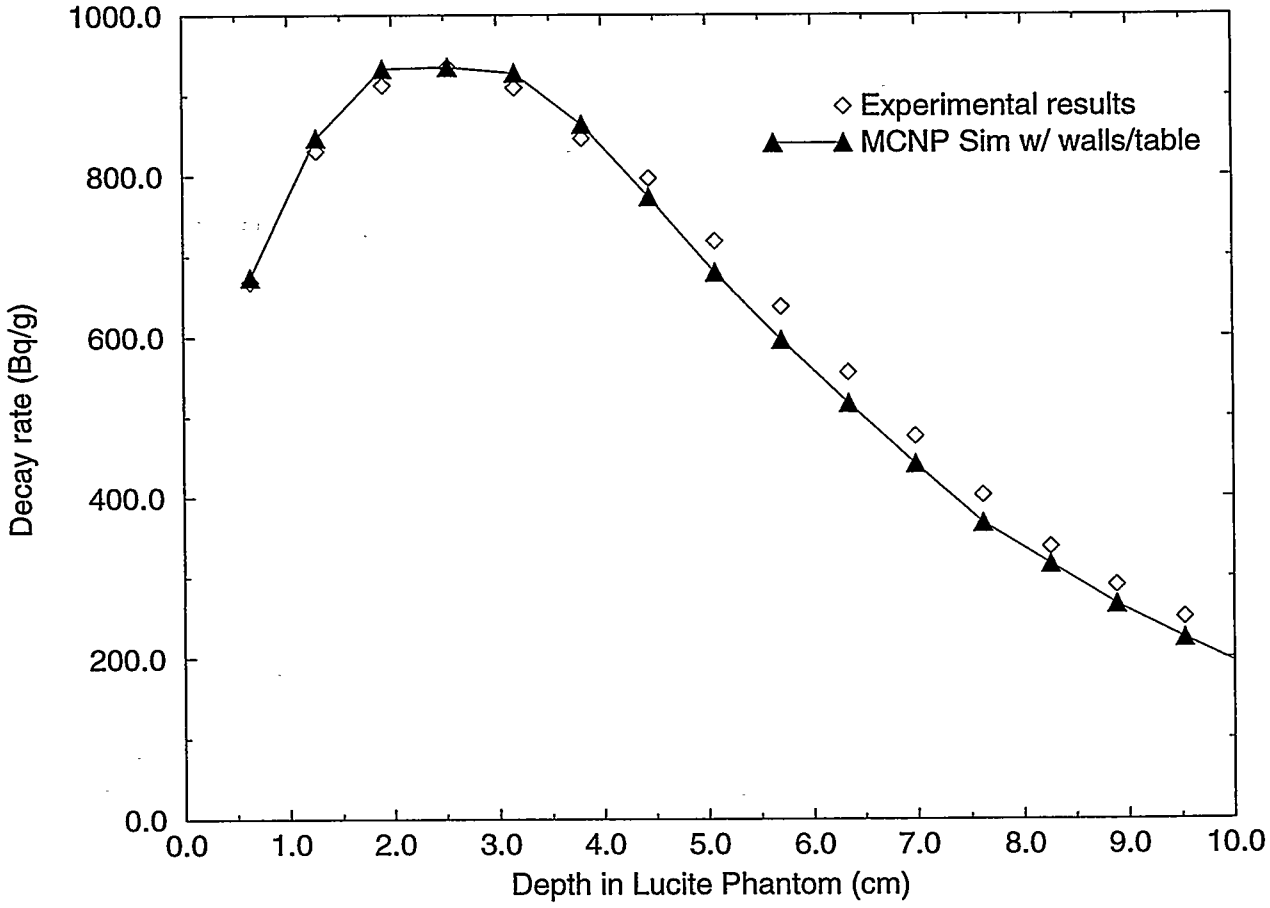

Figure 5: Normalized goil foil activation comparision. MCNP simulation results have been normalized to be equal to the maximum experimental data point at 2.54 cm.

demonstrates a reasonably good prediction of the slope of the foil activation with depth. The experiment yieldied a response that fell off less gradually than expected, but the maximum deviation was only 9%.

Results of the cross (lateral) foils at the three depths of interest are shown in Fig. 6. The MCNP predictions have been normalized as in Fig. 5. The most striking characteristic is the activity depression at the center of each cross. This is likely due to the flux depression along the centerline of the phantom due to absorbtion in the gold foils. Based on the thermal cross section of gold, it was not expected that the flux would be lowered along the centerline by more than a few percent, However, the 5 eV resonance in gold absorbed a significant fraction of the neutrons before thermalization. To more accurately measure the true thermal flux, fewer gold foils should be used. Also, subtracting the activation in a cadmium covered gold foil at the same depth as a foil of interest would correct for absorbtion of 5 eV neutrons.

The experimental data in Fig. 6 shows that for each cross, the activation is somewhat

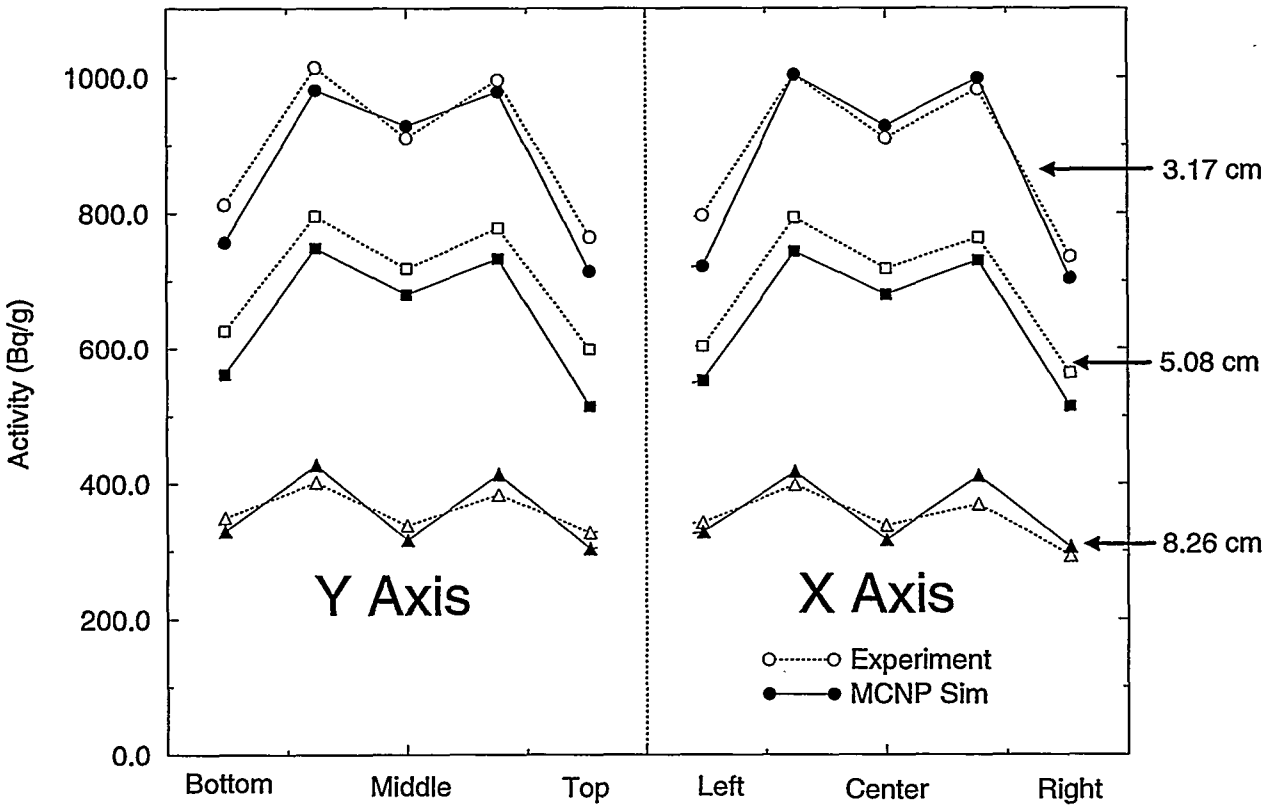

Figure 6: Comparison of activation of gold foils on crosses at 3.17 cm, 5.08 cm, and 8.26 cm. Note higher activations closest to left-side wall and to floor. MCNP values have been normalized at the 2.54 cm point as in Fig. 5

asymetric. This lends evidence to the room scatter effect, suggesting that the close left wall contributes a significant factor, as well as items underneath the apparatus, such as the table and floor.

4 Spectral Characterization

An attempt was made to characterize the in-air neutron spectrum using activation foils and a spectrum unfolding code. Preliminary estimates of the spectrum were modeled using MCNP and then combined with experimental data in SPECTRE[7] to unfold the neutron spectrum.

The experimental setup shown in Fig. 7 consisted of three cadmium disks containing six activation foils. The beam current provided by the 88-inch cyclotron was deemed too low to use thin foils ($\sim$ 0.1 mm). Foils used in this system were made as thick as 0.25 cm. This represents a significant difference and leads to the condition where the foils themselves may have influenced the spectrum significantly and thus biased the results.

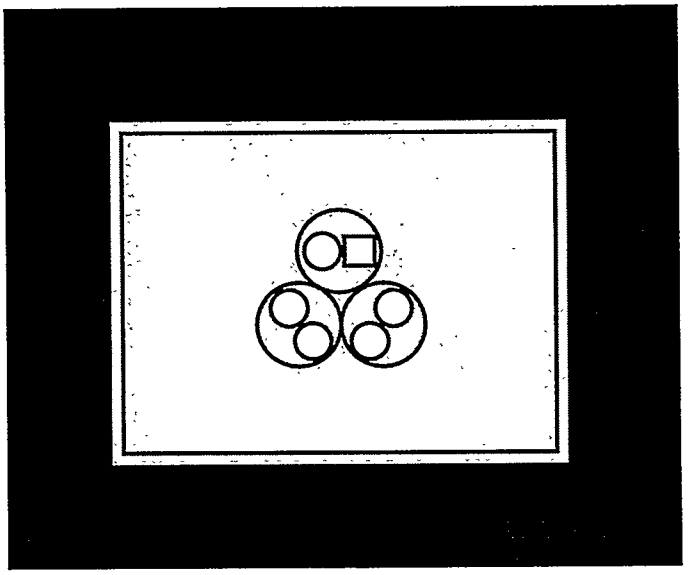

Figure 7: Activation Foil Geometry. Shaded circles indicate cadmium covers. The foils were placed on the Teflon moderator surface.

These disks were counted with a germanium gamma-ray spectrometer at the Low-Background Facility at a distance of 25 cm from the detector face. The detector was calibrated at this distance using a model 7600 multi-line source obtained from Isotope Products Inc. This source is $\pm 3\%$ traceable to NIST and provides absolute calibration of the detector efficiency over the energy range 59-1836 keV. Observed counting rates, branching ratios, and the detector absolute efficiency were used to calculate the activities produced.

Cadmium was used to remove thermal neutrons from the spectrum entering the foils. This isolates the epithermal resonances in each foil and makes the activation data independent of the 1/v cross section characteristic. Table 1 lists the foils used.

The cadmium covers were 10 cm in diameter and were 0.0254 cm thick. The foils were completely covered on all sides with cadmium. The foils were then arranged equidistant from the beam center on the exit side of the moderator.

MCNP was used to determine a-priori fluxes for input into SPECTRE. The experimental system was modeled using a modified version of the MCNP file described earlier. Tallies for volume averaged flux in each foil and flux multiplied by cross section were run with the model. This allowed for prediction of expected activation using MCNP as well as for preparing input data for SPECTRE.

SPECTRE is a spectral unfolding program developed at INEL. It uses a Gauss-Seidel iterative method to solve the system of equations provided by the activation data, preliminary flux esitimate, and cross section data. Using an initial flux estimate, SPECTRE iterates

Foil	Reaction	Resonance	Dimensions	Mass
Au	$^{197}Au(n,\gamma)^{198}Au$	5 eV	5 cm diameter disc	4.0 g
W	$^{186}W(n,\gamma)^{187}W$	18 eV	5 cm diameter disc	21.95 g
Co	$^{59}Co(n,\gamma)^{60}Co$	132 eV	5 cm diameter disc	57.6 g
Mn	$^{55}Mn(n,\gamma)^{56}Mn$	340 eV	5 cm diameter disc	16.7 g
Cu	$^{63}Cu(n,\gamma)^{64}Cu$	1 keV	5 cm diameter disc	60.5 g
In	$^{113}In(n,\gamma)^{114}In$	1 eV	2.5 cm x 2.5 cm sq.	11.2 g
In	$^{115}In(n,n')^{115m}In$	430 keV	2.5 cm x 2.5 cm sq.	11.2 g

Table 1: Activation Foils.

until it meets a predetermined convergence criteria. It is very important to have distinct resonances and good counting statistics when running this type of code. The initial flux estimate was provided by the volume averaged flux tally from the MCNP model.

Additionally, the cross-section data for each foil must be included in the input file. This data was gathered by tallying flux multiplied by cross section in a 120 group structure and then dividing the result by the flux in each material.

The activity predictions by MCNP are shown against the measured values in Table 2. The beam ran for 641 minutes generating a total yield of 1.63×10^{14} neutrons, as determined by the ^{7}Be activation measurements.

There was insufficient data to include activation due to the $^{115}In(n,n')$ reaction due to the low cross section combined with the low beam current. For three elements (W, Co, Mn), the calculated and measured activations matched quite closely. Two of the elements (In, Au) yielded measured activations that were somewhat higher than was expected. The resonances in these two materials correspond to the lowest energies of 1 eV and 5 eV. The higher measured activations were therefore consistent with the previous conclusion that thermal and near-thermal contamination due to room return was higher than expected. The most significant difference between the calculated and measured activation occured with ^{64}Cu, in which the measured activation was much lower than expected. It turns out that cadmium has a large series of resonances in the 1 keV range. Unfortunately, the copper resonance is of the similar magnitude as the cadmium resonance and appears to have been washed out, invalidating the copper activation data. Without a reliable value for the copper activation, it was not possible to calculate an informationally useful spectrum.

In Ref. [8], each reaction was measured up to four times. From these runs they extracted

Isotope	Calculated	Measured	Difference
^{187}W	1.05 x10^4	1.08 x10^4	+ 2.9%
^{114}In	1.63 x10^5	2.08 x10^5	+ 27.6%
^{198}Au	3.10 x10^4	3.98 x10^4	+ 28.4%
^{64}Cu	1.01 x10^4	0.64 x10^4	- 57.8%
^{59}Co	16.0	17.2	+ 7.5%
^{56}Mn	6.95 x10^4	6.81 x10^4	- 2.1%
^{115m}In	—	N/A	—

Table 2: Measured and Calculated Activities. Units are in decays/minute.

twenty-seven data points for the unfolding procedure. From these points, they were able to extract a reliable eight group spectrum. With the limit of only seven data points and reaction rates that are four or more orders of magnitude less than in Ref. [8], it is unrealistic to expect reliable results.

5 Conclusions

The in-phantom activation data supports the validity of our MCNP modeling. The remaining discrepancies will most likely disappear with more precise modeling of the experimental setup. At this point it is unclear if activation foils can be successfully used to characterize the in-air neutron spectrum. Further exploration of this technique should include other possible resonances such as that in ^{45}Sc.

6 Acknowledgements

We would like to thank D. Nigg for loaning us the Fluental blocks and the staff at the 88-inch cyclotron for their support.

References

[1] Ludewigt, B. A., Chu, W. T., Donahue, R. J., Kwan, J., Phillips, T. L., Reginato, L. L., and Wells, R. P., "An Epithermal Neutron Source for BNCT Based on an ESQ-

Accelerator," Proceedings of the Topical Meeting on Nuclear Applications of Accelerator Technology, 489-493, presented at the ANS Winter Conference in Albuquerque, NM, Nov. 16-20, 1997.

[2] Kwan, J. W., Anderson, O. A., Reginato, L. L., Yu, and S. S., "A 2.5 MeV Electrostatic Quadrupole DC-Accelerator for BNCT Applications," Nucl. Instrum. Methods B99, 710-712 (1995).

[3] Bleuel, D. L., Donahue, R. J., Ludewigt, B. A., and Vujic, J., "Designing Accelerator-based Epithermal Neutron Beams for Boron Neutron Capture Therapy," Medical Physics 25 (9), 1725-1734 (1998).

[4] Auterinen, I., and Hiismaki, P., "Design of an Epithermal Neutron Beam for the TRIGA Reactor in Otaniemi," Proceedings of the CLINCT BNCT Workshop, TKK-F-A718, Helsinki, 14-24, 1993.

[5] Briesmeister, J. F., MCNP - A General Monte Carlo N-Particle Transport Code, Version 4B, Los Alamos National Lab, 1997.

[6] Bleuel, D. L., Donahue, R. J., Ludewigt, B. A., and Vujic, J., "Development of a Neutron Energy-Biased In-Air Figure of Merit for Predicting In-Phantom BNCT Neutron Beam Characteristics," presented at the Eighth International Symposium on Neutron Capture Therapy for Cancer in La Jolla, CA, Sep. 13-18, 1998.

[7] Nigg, D. W., et. al., "INEEL BNCT Research Program Annual Report 1997," Appendix B., Venhuizen, J. R. (ed.).

[8] Nigg, D. W., Harker, Y. D., Hartwell, J. K., Wemple, C. A., "Collaborative Spectral Characterization of the Finnish Epithermal-Neutron Beam Facility for BNCT."